Desalination and Water Treatment
www.deswater.com

doi: 10.5004/dwt.2017.21492

92 (2017) 160–171
October

Improved electrocoagulation process using chitosan for efficient removal of cefazolin antibiotic from hospital wastewater through sweep flocculation and adsorption: kinetic and isotherm study

Saeid Ahmadzadeh[a,b,*], Ali Asadipour[c], Mehdi Yoosefian[d], Maryam Dolatabadi[e,*]

[a]*Neuroscience Research Center, Institute of Neuropharmacology, Kerman University of Medical Sciences, Kerman, Iran, Tel. +98 3431325241; Fax: +98 3431325215; email: chem_ahmadzadeh@yahoo.com (S. Ahmadzadeh)*
[b]*Pharmaceutics Research Center, Institute of Neuropharmacology, Kerman University of Medical Sciences, Kerman, Iran*
[c]*Department of Medicinal Chemistry, Faculty of Pharmacy, Kerman University of Medical Sciences, Kerman, Iran, email: aliasadipour@yahoo.com*
[d]*Department of Chemistry, Graduate University of Advanced Technology, Kerman, Iran, email: mahdi7462@gmail.com*
[e]*Environmental Science and Technology Research Center, Department of Environmental Health Engineering, Shahid Sadoughi University of Medical Sciences, Yazd, Iran, email: health.dolatabadi@gmail.com*

Received 26 February 2017; Accepted 26 September 2017

ABSTRACT

Recently widespread usage of cephalosporin antibiotics in medical and veterinary fields has received growing attentions as severe contaminants of aquatic ecosystems. Since there is no report on the removal of cefazolin (CFZ) using electrocoagulation and adsorption (EC/AD) coupling treatment process, the present work deals with efficient removal of CFZ from hospital wastewater using EC/AD process. To achieve the optimal condition, response surface methodology (RSM) was applied successfully with the removal efficiency of 100% under optimal operating condition of 7.8 pH, 15.5 mA cm^{-2} current density, 60 mg L^{-1} initial CFZ concentration, 1.0 cm inter-electrode distance, 0.7 g L^{-1} chitosan dosage and electrolyte dose of 0.07 M NaCl within the equilibrium treatment time of 23 min which is in adequate agreement with the predicted model using analysis of variance. Kinetic and isotherm models were studied to figure out the exact mechanism of the CFZ removal. Kinetic studies revealed that the second-order model (R^2 = 0.9715) best fitted with the experimental results. Langmuir isotherm model (R^2 = 0.9851) predicted the maximum adsorption capacity of 1,250 mg g^{-1}. The obtained results suggested that charge neutralization of the negatively charged CFZ through binding with cationic hydrolysis products and sweep flocculation as the determinant mechanisms control the adsorption of CFZ molecules on aluminum hydroxide precipitates. Under the optimal condition, electrode consumption and electrical energy consumption were found to be 0.024 g during a single run and 1.251 kWh m^{-3}, respectively. The predicted treatment model for the synthetic wastewater is in satisfactory agreement with removal efficiency of the hospital wastewater.

Keywords: Cefazolin; Hospital wastewater; Electrocoagulation; Adsorption; Chitosan; Response surface methodology

1. Introduction

Owing to the fact that the extensive use of pharmaceutical antibiotics for human therapy and farming industry, they have recognized as severe contaminants of surface water, groundwater and drinking water around the manufacturing communities, domestic zones as well as industrial farming areas [1]. Inappropriate disposal of unused or expired antibiotics causes incomplete metabolization in humans and on the other hand, their partial removal by conventional treatment technologies resulted in increasing antibiotics contamination in the last decades [2].

* Corresponding author.

Among cephalosporin antibiotics, due to the widespread usage of cefazolin (CFZ) in medical and veterinary fields, its residue level as a pharmaceutical contaminant in environmental media is relatively high which exhibited some harmful effects such as acute and chronic toxic effects on microbial activity. Moreover, owing to its poor biodegradable activity in the biological treatment process, CFZ disrupted the biological balance of aquatic ecosystems and on the other hand, resulted in developing the antibiotic resistance in microorganisms [3–5].

Due to the insufficient CFZ removal efficiency in conventional wastewater treatment plants, developing of alternative techniques for wastewater treatments before releasing them into the environment are highly desired. Literature survey revealed that a few studies have been carried out for removal of CFZ contamination from the aquatic environments including Fenton [6], O_3 and H_2O_2/O_3 [7], TiO_2/UV [8], coagulation [9] and adsorption [10]. The reported residual level of CFZ in hospitals wastewater is about 32 μg L^{-1} to 85.35 mg L^{-1} [6,11,12].

Electrocoagulation (EC) as an advanced economic and efficient technique among the other electrochemical treatment methods received an extensive practical application by providing a satisfactory result for the treatment of different wastewaters [13]. The scientific reports in last few years such as removal of dyes [14], heavy metal ions [15] and persistent organic compounds [16] revealed that EC technique comparatively guarantees better quality wastewater before its release into the aquatic environment. Due to the 'green technology' characteristics of EC process, the absence of harmful substances generation, producing low amount of TDS, comparatively low cost process and maintenance compared with the other mentioned techniques, interest in using EC process in industrial applications has been revived [17]. EC process involves three consecutive phases including generation of coagulants species in situ by electrolytic oxidation of the sacrificial metal anode such as aluminum, inconstancy of the contaminants where they are transformed into amorphous precipitates of adsorbed forms on hydroxides such as $Al(OH)^{2+}$, $Al(OH)_2^+$, $Al(OH)_3$ and Al^{3+}, suspension of the particulate and breaking of the emulsions and finally aggregation of the destabilized phases to form flocs. Besides the current studies in the field of electrochemistry, electrochemical sensors indicated a rapidly growing scientific field in environmental and biological monitoring investigations for quantitative determination of contaminants [18–23].

On the other hand, another appropriate alternative for treatment of wastewater namely adsorption has been found to be beneficial along with EC technique to achieve higher removal efficiency in wastewater treatment process. Throughout the adsorption process, the contaminants physically or chemically are adsorbed onto the surface of the adsorbent molecules. During the last decades, great attempts have been done to find suitable and affordable adsorbents such as bagasse, zeolite, fly ash, sawdust and chitosan for wastewater treatments [24]. Chitosan as a natural polysaccharide is considered the largest biomaterial after cellulose and used as an adsorbent in the medical field and food industries [2]. Chitosan generates from chitin which is the structural element found in the exoskeleton of crustaceans such as shrimps, lobsters and crabs. Also, it occurs naturally in some microorganisms such as fungi and yeast. Even though its structure is similar to cellulose, but also it contains acetylamine or free amino groups which improve its properties as an adsorbent.

It is important to note the removal of CFZ contaminant by EC/AD coupling process has not been previously considered, the current work deals with the feasibility of the CFZ removal from hospital wastewater using chitosan as adsorbent via a combined EC sorption. The effects of various operating parameters such as electrolyte type and concentration, inter-electrode distance, initial CFZ concentration, pH, current density, reaction time and chitosan dosage were investigated to achieve the best efficient and economical removal condition. Moreover, the first- and second-order kinetics models were studied in the optimum operating condition. Consequently, two common adsorption isotherms namely Freundlich and Langmuir were used to checking out the exact mechanism of CFZ adsorption.

2. Materials and methods

2.1. Chemicals

CEZ ($C_{14}H_{14}N_8O_4S_3$, 454.51 molecular weight) was purchased from Sigma-Aldrich, Kuala Lumpur, Malaysia. The mobile phase was prepared using HPLC grade acetonitrile and deionized water. Electrolytes including NaCl, KCl, KNO_3, NH_4Cl, Na_2SO_4 and $CaCl_2$ were purchased from Merck Company, Malaysia. Hydrochloric acid and sodium hydroxide from Sigma-Aldrich were used for pH adjustments. All reagents used are analytical reagent grade with the highest available purity which used without any further purification except for vacuum drying over P_2O_5. All the solutions were prepared using deionized water.

2.2. Preparation of the chitosan adsorbent

Shrimp wastes (SW) were obtained from local markets of Kerman city, Iran. The SW was washed to remove loose tissue and adhered dirt and dried in sunlight for 1–2 d. The dried SW was fed to a grinder and grounded. The grounded SW was transferred to demineralization, deproteinization and deacetylation steps. Demineralization of SW was carried out in the solution of 1.0 M HCl (1:20 W/V) for 24 h under stirring at room temperature. To deproteinized the demineralized shells, they were poured into the solution of 1.0 M NaOH in the ratio of 1:20 (W/V) and maintained for 24 h under stirring at room temperature. The obtained product was chitin. Deacetylation of chitin was carried out using a solution of 50% NaOH with the ratio of 1:20 (W/V) for 2 h at 100°C. The resulting solid was filtrated by Whatman filter number 1 and was washed thoroughly with distilled water to neutralize and dry at room temperature for 24 h. Consequently, it was dried in an oven at 60°C for 4 h finally [25,26]. The pH_{pzc} value of chitosan was determined to explain the adsorption behavior. This parameter reveals the characteristics of surface active sites depend on solution pH. The pH_{pzc} of chitosan was found to be around 6.5, implying that the surface of adsorbent would be positively charged at lower pH and negatively charged at higher pH.

2.3. Experimental procedure

All experiments were conducted in batch mode by Plexiglas electrochemical cell with dimensions of 12 × 5 × 5 cm

to hold a sample of 250 mL using two aluminum plate electrodes with immersed dimensions of 3 × 2 × 0.2 cm. The pH adjustment was carried out by adding small volumes of 0.01 N of HCl or NaOH to the solutions and measured using Metrohm 827 pH/mv meter. KNAUER Smartline HPLC (C_{18} column; 250 × 4.6 × 5 mm) with a UV detector was used at a wavelength of 272 nm for quantitative determination of residual CFZ. A mixture of H_2O and acetonitrile with a ratio of 78/22 (vol%) was applied as mobile phase with an injection flow rate of 1 mL min^{-1}. Removal efficiency of CFZ was calculated by the following equation [27]:

$$\%\text{Removal CFZ} = \frac{C_0 - C_t}{C_0} \times 100 \quad (1)$$

where C_0 and C_t (mg L^{-1}) denote the concentration of CFZ before and after EC/AD process and time t, respectively.

2.4. Statistical design

Central composite design (CCD) was applied to optimize the experimental conditions under response surface methodology (RSM) using Design Expert 7 software. In the present work, the CCD consists of 2^n factorial points, $2n$ axial points and moreover a given number of center points, where n is equal to 5 which is the number of numeric factors including initial CFZ concentration, solution pH, current density, reaction time and chitosan dosage. The investigated factors and levels of each factor are presented in Table 1. Experimental data from the CCD was analyzed and fitted to a second-order polynomial model expressed as follows:

$$Y = \beta_0 + \sum_{i=1}^{n} \beta_i X_i + \sum_{i=1}^{n} \beta_{ii} X_i^2 + \sum_{i=1}^{n-1} \sum_{j=i+1}^{n} \beta_{ij} X_i X_j \quad (2)$$

where Y, β_0, β_i, β_{ii}, β_{ij}, X_i and X_j denote the predicted response of CFZ removal, the intercept parameter, the linear coefficients, the quadratic coefficients, the interaction coefficients and the coded values of independent factors, respectively.

2.5. Kinetic and isotherm studies

Since the Freundlich adsorption isotherm could be applied over a wide range of concentrations and can provide a satisfactory fitting of the experimental data with calculated theoretical data, investigated in the current work. The effect of several parameters such as surface heterogeneity, the exponential distribution of the active sites and their energy are considered through the experimental model. The Freundlich isotherm, a reversible adsorption, is not restricted to the formation of a monolayer. The linear model of Freundlich isotherm is described by the following equation [28–30]:

$$\log q_e = \log K_f + \left(\frac{1}{n}\right) \log C_e \quad (3)$$

where K_f, n and C_e based on mg L^{-1} are Freundlich constant related to adsorption capacity, the energy or intensity of adsorption and the equilibrium concentration of the contaminant.

Langmuir isotherm, an adsorption model, is valid for a monolayer deposition of adsorbates on the homogeneous surface of the adsorbents with a finite number of identical sites. The linear model of Langmuir isotherm is expressed as follows [24,28]:

$$\frac{C_e}{q_e} = \frac{C_e}{q_m} + \frac{1}{bq_m} \quad (4)$$

where q_e, q_m, b and C_e are the amount of adsorbed contaminant, the Langmuir constant representing maximum monolayer adsorption capacity, the Langmuir constant related t_0 the energy of adsorption and equilibrium concentration of contaminant, respectively. The dimensionless constant of RL as the important feature of the Langmuir isotherm can be described as follows [24,31]:

$$\text{RL} = \frac{1}{(1 + bC_0)} \quad (5)$$

where RL, b and C_0 are the equilibrium constants which indicates the type of adsorption, Langmuir constant and various concentration of contaminant solution, respectively. The RL values between 0 and 1 indicate the favorable adsorption.

To investigate the kinetics of the removal process the first- and second-order kinetics models were studied. The first-order kinetics model can be declared as follows [28]:

$$\log(q_e - q_t) = \log(q_e) - k_1 t/2.303 \quad (6)$$

where q_e and q_t based on mg g^{-1} are the adsorption capacity at equilibrium time and t time (min), respectively. k_1 (min^{-1}) is the constant of first-order adsorption.

Moreover, the second-order kinetics model can be expressed as follows:

$$\frac{t}{q_t} = \frac{1}{k_2 q_e^2} + \frac{t}{q_e} \quad (7)$$

Table 1
Coded and actual values of numeric factors

Coded variables (X_i)	Factors (U_i)	Experimental field				
		$-\alpha$	–1 level	0	+1 level	$+\alpha$
X_1	A = initial CFZ concentration (mg L^{-1})	20	57.77	85	112.32	150
X_2	B = solution pH	4	5.73	7	8.26	10
X_3	C = current density (mA cm^{-2})	5	9.34	12.5	15.65	20
X_4	D = reaction time (min)	5	12.24	17.5	22.75	30
X_5	E = chitosan dosage (g L^{-1})	0	0.29	0.5	0.71	1

where q_e and q_t based on mg g^{-1} are the adsorption capacity on aluminum hydroxide at the equilibrium time and t time (min), respectively. k_2 (g mg^{-1} min^{-1}) is the constant of the second-order adsorption.

2.6. Electrical energy and electrode consumption studies

The amount of aluminum electrode consumption during the EC/AD process under the optimal condition can be expressed as follows [27]:

$$\mathrm{ELC} = \left(\frac{ItM}{nF}\right) \tag{8}$$

where I, t, M, n and F denote applied electrical current (A), reaction time (s), molecular mass (g mol^{-1}), the number of electrons and Faraday constant (96,485 C mol^{-1}), respectively.

Moreover, the amount of electrical energy consumption during EC/AD process under optimal condition can be expressed as follows [27]:

$$\mathrm{EEC} = \left(\frac{UIt}{V}\right) \tag{9}$$

where U, I, t and V denote applied voltage (V), applied electrical current (A), reaction time (h) and volume of sample (L), respectively.

On the other hand, the current efficiency (ϕ) of EC/AD process was expressed by following equation based on the comparison of weight loss of aluminum electrodes (ΔM_{exp}) during EC/AD process with theoretical amount of aluminum electrodes dissolution (ΔM_{theo}) [31]:

$$\varphi = \frac{\Delta M_{exp}}{\Delta M_{theo}} \times 100 \tag{10}$$

The specific electrical energy consumption (SEEC) was described as a function of aluminum electrode weight consumed during EC/AD process in kWh (kg Al)$^{-1}$ and can be expressed by the following equation [27]:

$$\mathrm{SEEC} = \frac{nFU}{3.6 \times 1{,}000 M\varphi} \tag{11}$$

3. Results and discussion

3.1. Preliminary evaluation of electrocoagulation process

The effect of electrolyte type and concentration on CFZ removal efficiency was investigated. The solutions of 0.07 M electrolytes were used to investigate the effect of electrolyte type on the removal efficiency. The maximum removal was obtained using NaCl as the electrolyte at equilibrium time of 25 min (Fig. 1). Literature surveys revealed that addition of appropriate electrolyte significantly improved the efficiency of EC/AD process due to increasing the conductivity of the wastewater which affects the Faradic yield, cell voltage and consequently energy consumption of the process.

The presence of NaCl electrolyte plays an important role to overcome the adverse effects of other anions such as CO_3^{2-}, HCO_3^- and SO_4^{2-} which may result in precipitation of Ca^{2+} cations as an insulating layer on the surface of the cathode and increasing the ohmic resistance of the EC/AD cell [27,31]. However, the extra amount of NaCl caused irregular dissolution of Al electrode; therefore, the electrolyte doses of the NaCl (0.01–0.1 M) were optimized and presented in Fig. 2. The obtained results revealed that the removal efficiency of CFZ remained almost unchanged in the range of 0.07–0.1 M of electrolyte dose. Therefore, NaCl electrolyte with the optimized concentration of 0.07 M was used for further studies.

Furthermore, the effect of inter-electrode distance on the removal efficiency of CFZ was investigated. It is known that the drop in ohmic potential of the EC cell is proportional to the inter-electrode spacing and on the other hand the distance between electrodes affects the electrolysis energy consumption especially when sample conductivity is low. To determine the effect of the inter-electrode distance the distance between electrodes was changed in the range of 1.0–3.0 cm. Current density loading of 12.5 mA cm^{-2}, initial CFZ 50 mg L^{-1}, chitosan dosage 0.5 g L^{-1} and pH 7.5 was kept constant. The obtained results revealed that the lowest residual

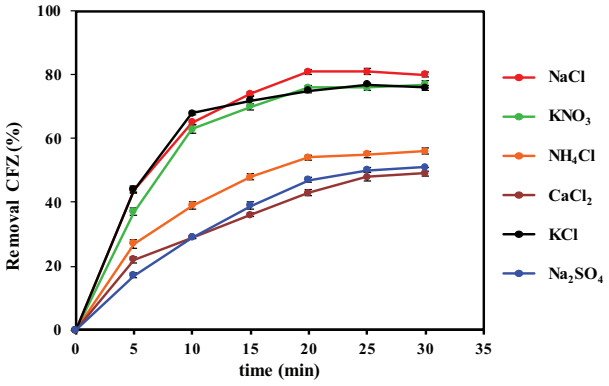

Fig. 1. Effect of electrolyte type; CFZ concentration 100 mg L^{-1}, current density 12 mA cm^{-2}, solution pH at 7.5, inter-electrode distance 1.0 cm, chitosan dosage 0.5 g L^{-1} and concentration of electrolyte 0.07 M.

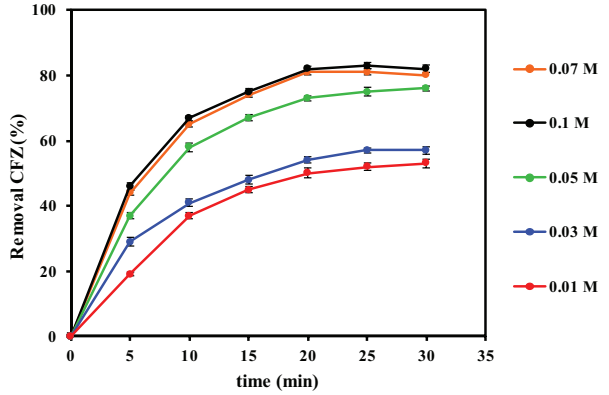

Fig. 2. Effect of electrolyte dose; CFZ concentration 100 mg L^{-1}, current density 12 mA cm^{-2}, solution pH at 7.5, chitosan dosage 0.5 g L^{-1} and inter-electrode distance 1.0 cm.

CFZ concentration was 7.0 mg L^{-1} at the inter-electrode distance of 1 cm. At the inter-electrode distance of 1.5, 2, 2.5 and 3 cm, residual CFZ concentrations of 11.35, 19.14, 26.5 and 33.5 mg L^{-1} were obtained, respectively. The obtained results, in accordance with the other reports, show that by reducing the inter-electrode distance, the resistance of motion reduced. The observed behavior can be attributed to the shorter travel path. Consequently, the electrical energy consumption was decreased and efficiency of the process improved [27,31].

After optimizing the abovementioned parameters in preliminary evaluation of EC process, in the second step, RSM design was applied to optimize the other main parameters through EC/AD process. The experimental conditions along with the obtained results of 50 runs according to RSM design are summarized in Table 2. As it can be seen, the removal efficiency of CFZ changed from 47.15% to 100.00%.

3.2. Fitting of the process model and statistical analysis

To evaluate the effects of independent factors including initial CFZ concentration, solution pH, current density, reaction time and chitosan dosage on removal efficiency of CFZ, 50 runs were carried out by RSM. To obtain the regression equation experimental results were fitted to the quadratic model. The quadratic polynomial model in term of significant coded factors (terms with P value ≤ 0.05) is expressed as follows:

$$\begin{aligned}\text{Removal}(\%) = {} & 82.36 - 5.27X_1 + 4.03X_2 + 5.41X_3 \\ & + 4.85X_4 + 5.33X_5 + 1.71X_2X_4 - 1.38X_2X_5 \\ & - 1.77X_3X_5 - 5.02X_2^2 - 1.90X_4^2\end{aligned} \quad (12)$$

where X_1, X_2, X_3, X_4 and X_5 are initial CFZ concentration, solution pH, current density, reaction time and chitosan dosage, respectively. The adequacy of model checked and the obtained results summarized in Table 3.

According to Table 3, the analysis of variance (ANOVA) test confirmed that the applied quadratic model was significant with 95% confidence level and F value of 49.02. Since the amount of P value probability was >0.05, no evidence of lack of fit for the model was observed. Furthermore, the values of the correlation coefficient (R^2), adjusted correlation coefficient (adj. R^2) and predicted correlation coefficient (pred. R^2) were found to be 0.9263, 0.9074 and 0.8526, respectively, which indicates the experimental and model predicted values are in good agreement. Moreover, the obtained amount of 30.20 for adequate precision which is more than 4 indicates an adequate signal to noise ratio.

3.3. Pareto analysis

Graphical Pareto analysis provides noteworthy information about the importance of the operational parameters to interpret the obtained results. Pareto analysis indicates the percentage effect of each factor on the CFZ removal efficiency as the response, according to the equation expressed as follows:

$$P_i = \frac{b_i^2}{\sum b_i^2} \times 100 \quad (i \neq 0) \quad (13)$$

where b_i represents the estimation of the significant effect of the operational parameters. As it can be seen from Fig. 3, the contributions of the operational parameters (X_1, X_2, X_3, X_4 and X_5) on the percentage of CFZ removal efficiency are 17.50%, 10.03%, 18.08%, 14.53% and 17.53%, respectively. Moreover, the contribution of the interaction effect (X_2X_4, X_2X_5 and X_3X_5) on the percentage of CFZ removal was found to be 1.80%, 1.18% and 1.93%, respectively. The contributions of the quadratic effects of (X_2^2 and X_4^2) on the CFZ removal efficiency were found to be 15.53% and 2.22%, respectively. The obtained results revealed that, among all factors, initial concentration (X_1), current density (X_3), chitosan dosage (X_5) and quadratic effects of pH (X_2^2) have the highest contribution to the removal efficiency of CFZ contaminant.

3.4. Electrocoagulation experiments

According to Eq. (3), it can conclude that the average value for CFZ removal efficiency is 82.36% when all operational parameters fixed at their center point values. Since the magnitude of the coefficient in front of each term shows the importance degree of that term, the most influencing terms among the significant operational parameters were found to be current density, followed by chitosan dosage, initial CFZ concentration, reaction time and pH, respectively. Moreover, it can be concluded that the removal efficiency of CFZ increased 10.82% (2 × 5.41) by increasing its current density from 9.36 (–1 level) to 15.65 mA cm^{-2} (+1 level). However, the removal efficiency decreased 10.54% (2 × 5.27) when initial CFZ concentration increased from 57.67 mg L^{-1} (–1 level) to 112.33 mg L^{-1} (+1 level).

The obtained results revealed that increasing the initial concentration of the CFZ contaminant resulted in decreases of removal efficiency of CFZ. As it can be seen from Fig. 4 that at the center point of the mentioned significant operational parameters including 12.5 mA cm^{-2} current density, 7.0 pH, 17.5 min reaction time and 0.5 g chitosan dosage, the removal efficiency of CFZ decreases from 87.62% to 77.08% by increasing its concentration from 57.5 to 112.33 mg L^{-1}. It is probably owing to the fact that the number of the formed metal hydroxide flocs was not sufficient for sedimentation the greater number of the CFZ molecules.

To investigate the effect of pH on the removal efficiency of CFZ, the EC processes carried out over the wide pH range of 4.0–10.0. The combined effects of the solution pH and CFZ concentration on the removal efficiency was depicted by the 3D surface plot (Fig. 5).

As is illustrated in Fig. 5, CFZ removal efficiency improved by increasing the pH and the maximum removal efficiency occurred at pH value of 7.80. Evidently, the effect of pH on the removal efficiency rate is higher in the range of 5.5–7.8 in comparison with 7.8–8.2. Moreover, at low initial pH condition, the aluminum hydroxides are soluble and are not able to absorb the pollutants. The obtained results were in accordance with other reported works using Al as the sacrificed electrode [25,32].

The effect of current density on the removal efficiency of CFZ contaminant was investigated and presented in Fig. 6. The removal efficiency of CFZ increased from 76.94% to 87.76% by increasing the current density from

Table 2
Experimental results of CFZ removal as a function of coded and actual values of four factors in CCD matrix

Run	Actual values					Coded values					CFZ removal (%)
	A (mg L^{-1})	B	C (mA cm^{-2})	D (min)	E (g L^{-1})	X_1	X_2	X_3	X_4	X_5	
1	57.67	8.26	15.65	12.24	0.29	–1	1	1	–1	–1	79.85
2	112.33	5.74	15.65	12.24	0.29	1	–1	1	–1	–1	67.78
3	85.00	7.00	12.50	17.50	0.00	0	0	0	0	–2.38	61.44
4	57.67	5.74	15.65	12.24	0.71	–1	–1	1	–1	1	80.35
5	57.67	8.26	15.65	22.76	0.71	–1	1	1	1	1	100.00
6	112.33	8.26	15.65	12.24	0.71	1	1	1	–1	1	74.50
7	20.00	7.00	12.50	17.50	0.50	–2.38	0	0	0	0	100.00
8	85.00	7.00	12.50	17.50	0.50	0	0	0	0	0	83.20
9	112.33	5.74	15.65	22.76	0.29	1	–1	1	1	–1	66.45
10	85.00	7.00	12.50	17.50	0.50	0	0	0	0	0	84.46
11	112.33	8.26	15.65	22.76	0.71	1	1	1	1	1	86.45
12	112.33	5.74	15.65	12.24	0.71	1	–1	1	–1	1	69.54
13	57.67	5.74	15.65	12.24	0.29	–1	–1	1	–1	–1	74.45
14	85.00	7.00	12.50	17.50	0.50	0	0	0	0	0	83.42
15	112.33	5.74	9.35	22.76	0.71	1	–1	–1	1	1	73.45
16	85.00	7.00	5.00	17.50	0.50	0	0	–2.38	0	0	59.45
17	112.33	8.26	9.35	12.24	0.71	1	1	–1	–1	1	68.50
18	85.00	7.00	12.50	17.50	0.50	0	0	0	0	0	78.00
19	57.67	5.74	15.65	22.76	0.29	–1	–1	1	1	–1	77.37
20	57.67	8.26	15.65	22.76	0.29	–1	1	1	1	–1	98.45
21	112.33	8.26	15.65	22.76	0.29	1	1	1	1	–1	82.50
22	57.67	5.74	9.35	12.24	0.29	–1	–1	–1	–1	–1	63.45
23	85.00	7.00	12.50	17.50	0.50	0	0	0	0	0	79.24
24	85.00	4.00	12.50	17.50	0.50	0	–2.38	0	0	0	47.15
25	57.67	5.74	9.35	22.76	0.29	–1	–1	–1	1	–1	65.58
26	112.33	8.26	9.35	22.76	0.29	1	1	–1	1	–1	72.40
27	57.67	8.26	9.35	22.76	0.29	–1	1	–1	1	–1	82.50
28	112.33	8.26	15.65	12.24	0.29	1	1	1	–1	–1	75.50
29	85.00	7.00	12.50	17.50	0.50	0	0	0	0	0	82.78
30	57.67	8.26	9.35	12.24	0.71	–1	1	–1	–1	1	83.74
31	57.67	5.74	15.65	22.76	0.71	–1	–1	1	1	1	88.42
32	57.67	5.74	9.35	12.24	0.71	–1	–1	–1	–1	1	73.45
33	112.33	5.74	15.65	22.76	0.71	1	–1	1	1	1	84.45
34	85.00	7.00	12.50	17.50	1.00	0	0	0	0	2.38	95.25
35	57.67	8.26	15.65	12.24	0.71	–1	1	1	–1	1	85.57
36	112.33	5.74	9.35	12.24	0.29	1	–1	–1	–1	–1	50.45
37	85.00	10.00	12.50	17.50	0.50	0	2.38	0	0	0	56.38
38	85.00	7.00	12.50	17.50	0.50	0	0	0	0	0	82.45
39	85.00	7.00	12.50	17.50	0.50	0	0	0	0	0	80.18

(Continued)

Table 2 *(Continued)*

Run	Actual values					Coded values					CFZ removal (%)
	A (mg L^{-1})	*B*	*C* (mA cm^{-2})	*D* (min)	*E* (g L^{-1})	X_1	X_2	X_3	X_4	X_5	
40	57.67	8.26	9.35	22.76	0.71	–1	1	–1	1	1	94.28
41	112.33	8.26	9.35	22.76	0.71	1	1	–1	1	1	81.45
42	112.33	8.26	9.35	12.24	0.29	1	1	–1	–1	–1	61.48
43	85.00	7.00	20.00	17.50	0.50	0	0	2.38	0	0	97.46
44	85.00	7.00	12.50	5.00	0.50	0	0	0	–2.38	0	55.84
45	57.67	5.74	9.35	22.76	0.71	–1	–1	–1	1	1	81.21
46	112.33	5.74	9.35	12.24	0.71	1	–1	–1	–1	1	69.45
47	112.33	5.74	9.35	22.76	0.29	1	–1	–1	1	–1	57.44
48	57.67	8.26	9.35	12.24	0.29	–1	1	–1	–1	–1	68.78
49	150.00	7.00	12.50	17.50	0.50	2.38	0	0	0	0	69.45
50	85.00	7.00	12.50	30.00	0.50	0	0	0	2.38	0	83.00

Table 3
ANOVA results for response surface of quadratic model

Response	Source	Analysis of variance				
		Sum of square	Degrees of freedom	Mean square	*F* value	*P* value Prob > *F*
CFZ removal (%)	Model	7,256.82	10	725.68	49.02	<0.0001
	Residual	577.33	39	14.80	–	–
	Lack of fit	540.73	32	16.90	3.23	0.0556
	Pure error	36.60	7	5.23	–	–

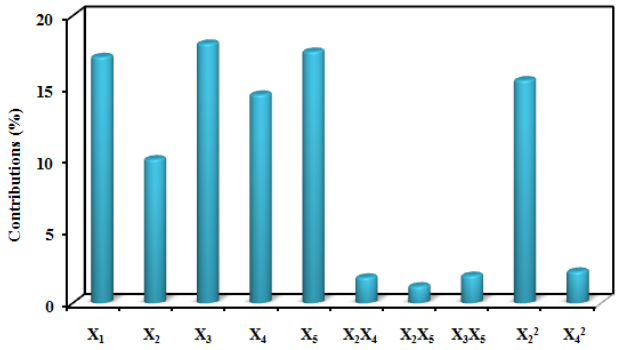

Fig. 3. Graphical Pareto analysis of the significant parameters on CFZ removal.

9.35 to 15.65 mA cm^{-2} at the center point of the significant operational parameters including 85 mg L^{-1} CFZ concentration, 7.0 pH, 0.5 g L^{-1} chitosan dosage and 17.5 min reaction time.

Current density as a significant operational parameter can affect the efficiency of the EC/AD process by controlling the concentration of the generated Al^{3+} and OH^-, the production rate of metal hydroxide as a coagulant, production rate of bubbles, size and growth of the flocs, for sedimentation of the CFZ contaminants. According to the obtained results presented in Fig. 7, the reaction time of the EC/AD process can affect the removal efficiency of CFZ contaminant.

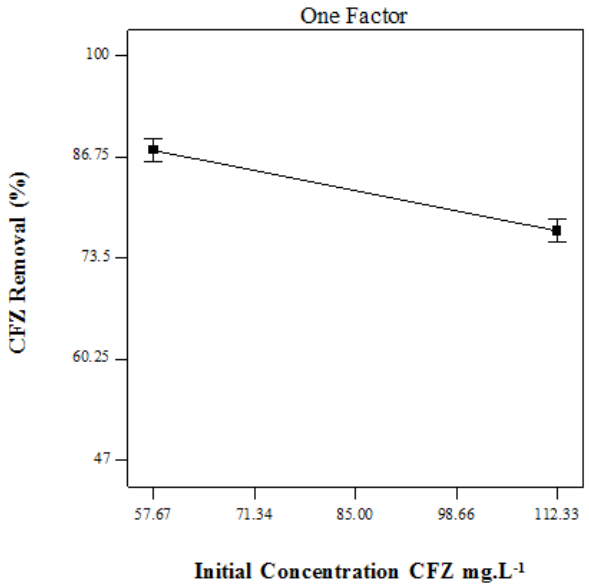

Fig. 4. Percentage of CFZ removal as a function of initial CFZ concentration; solution pH 7, current density 12.5 mA cm^{-2}, reaction time 17.5 min and chitosan dosage 0.5 g L^{-1}.

As it can be seen the removal efficiency of CFZ increased from 75.6% to 85.31% by increasing the reaction time from 12.24 to 22.76 min in the constant value of 85 mg L^{-1} CFZ

concentration, 7.0 pH, 10 mA cm^{-2} current density and 0.5 g L^{-1} chitosan dosage as the center points of the significant operational parameters. The observed curvature in the plot indicates that there is an optimum range of 20–22.7 min for reaction time with the maximum value of approximately 22.7 min, however, beyond the optimum electrolysis time the removal rate decreased as a result of the desorption phenomenon. The reaction time of 22.7 min which is required to reach the equilibrium remains unaltered at different CFZ concentration from 20 to 150 mg L^{-1}.

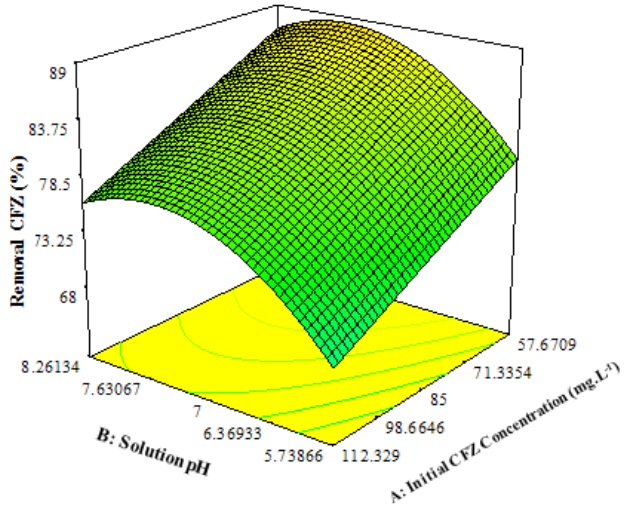

Fig. 5. 3D surface plot of CFZ removal percentage as a function of initial CFZ concentration and solution pH; current density 12.5 mA cm^{-2}, reaction time 17.5 min and chitosan dosage 0.5 g L^{-1}.

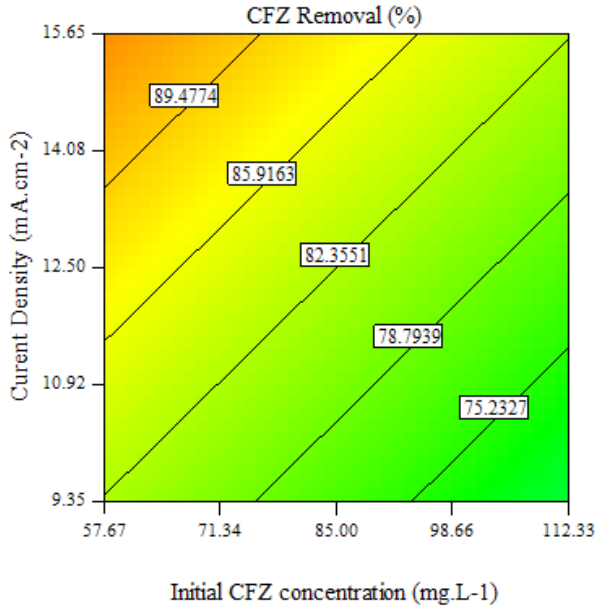

Fig. 6. Percentage of CFZ removal as a function of current density and initial CFZ concentration; solution pH at 7, chitosan dosage 0.5 g L^{-1} and reaction time 17.5 min.

The role of chitosan dosage on the process presented in Fig. 8. There is a direct relationship between the amount of chitosan dosage added and removal rate of CFZ contaminant. As it is demonstrated in Fig. 8, in the constant value of 85 mg L^{-1} CFZ concentration, 7.0 pH, 12.5 mA cm^{-2} current density and 17.5 min reaction time which is the center point of the mentioned parameters, the removal efficiency of CFZ increased from 76.02% to 87.68% by increasing the chitosan dosage from 0.29 to 0.71 g L^{-1}.

It is important to note that the removal efficiency of 98% achieved for only 1 g L^{-1} of chitosan dosage by applying the current density of 12.5 mA cm^{-2}. The removal efficiency was

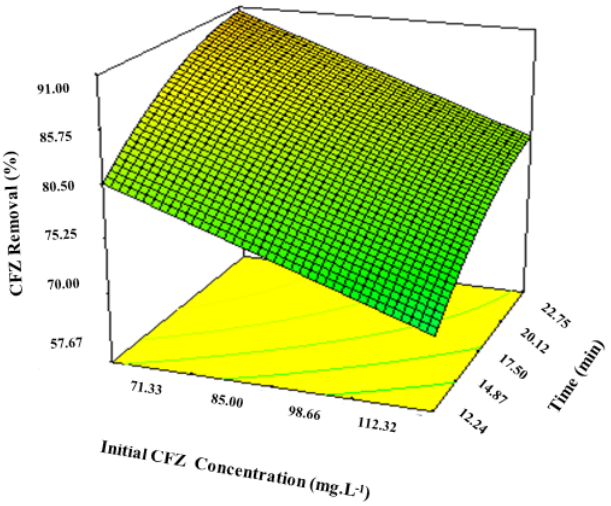

Fig. 7. 3D surface plot of CFZ removal percentage as a function of reaction time and initial CFZ concentration; solution pH at 7, chitosan dosage 0.5 g L^{-1} and current density 12.5 mA cm^{-2}.

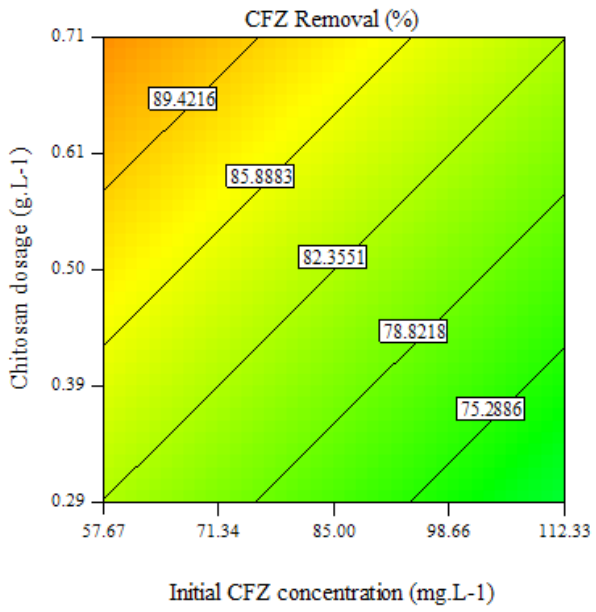

Fig. 8. Percentage of CFZ removal as a function of chitosan dosage and initial CFZ concentration; solution pH at 7, reaction time 17.5 min and current density 12.5 mA cm^{-2}.

significantly improved when coupling the two EC/AD process demonstrating that CFZ removal could result in fact from several complex mechanisms such as chemical precipitation and adsorption that simultaneously take place on the chitosan as well as on the formed flocs under EC [17]. Thus, it can be stated that the removal of CFZ in the EC/AD process resulted from synergistic effects of each individual CFZ removal process.

3.5. EC/AD process optimal condition

To find the optimum condition the optimization criteria for the main parameters including initial CFZ concentration, solution pH, current density, reaction time and chitosan dosage were adjusted to 'in range' level in the software and the removal efficiency of CFZ as the response was adjusted to 'maximize' level. From the recommended optimum conditions the best one which has the superior desirability of 0.998 and maximum CFZ removal of 100% was selected as the final optimal condition. The obtained values for the optimized parameters were pH 7.8, inter-electrode distance 1 cm, reaction time 23 min, current density 15.5 mA cm^{-2}, chitosan dosage 0.7 g L^{-1} and electrolyte dose of 0.07 M NaCl with the initial CFZ concentration of 60 mg L^{-1}. The obtained experimental value for CFZ removal efficiency and predicted value by the model were 100% and 99.71%, respectively (Table 4). It can be concluded that there is a satisfactory agreement between the experimental CFZ removal efficiency and the estimated value by the quadratic model. Hence, it confirmed the accuracy and precision of the designed model in the successful prediction of CFZ removal efficiency.

3.6. Removal mechanism of CFZ through EC/AD process

Al^{3+} ions which generated electrochemically from the sacrificial anode can go through the hydrolysis process at higher pH condition to produce a series of activated intermediates including $Al(OH)^{2+}$ and $Al(OH)_2^+$ that are able to destabilize the negatively charged CFZ molecules existed in the wastewater [33]. As it can be seen from the reactions below the destabilized particles then aggregate to form flocks:

Cathode reaction:

$$2H_2O + 2e^- \rightarrow H_2(g) + 2OH^- \quad \text{(I)}$$

Anode reaction:

$$Al \rightarrow Al^{3+} + 3e^- \quad \text{(II)}$$

In the solution:

$$Al^{3+}(aq) + 3H_2O \rightarrow Al(OH)_3 + 3H^+(aq) \quad \text{(III)}$$

$$nAl(OH)_3 \rightarrow Al_n(OH)_{3n} \quad \text{(IV)}$$

The generated $Al(OH)^{2+}$ as the cationic hydrolysis product and formed polymeric cationic species are able to remove the contaminant by adsorption and neutralization of the negatively charged CFZ. Adsorption of pollutant molecules on metal hydroxide precipitates, which is known as 'sweep flocculation' mechanism controlled the efficient removal of CFZ contaminant.

3.7. Kinetic modeling

First- and second-order kinetic models studied in the current work in the optimum condition of 60 mg L^{-1} CFZ concentration, 15.5 mA cm^{-2} current densities, 7.8 pH solution, 0.7 g L^{-1} chitosan dosage, 0.07 M NaCl as concentration and type of electrolyte and 1 cm inter-electrode distance. As it can be seen from Fig. 9 a linear relationship with the correlation coefficient of 0.7414 observed between $\log(q_e - q_t)$ and t. The kinetic data fitted to the first-order model equation and the amount of calculated k_1 presented in Table 5.

Moreover, the kinetic data fitted to the second-order model equation. The equilibrium adsorption capacity, q_e, and k_2 were calculated and summarized in Table 5. As it is illustrated in Fig. 10, the plot of t/q_t vs. t for CFZ adsorption was found to be linear with satisfactory correlation coefficients of 0.9715. It can be concluded that the obtained experimental

Table 4
Optimal condition and comparison between actual value and predicted value

Parameters	Optimal value
Type of electrolyte	NaCl
Electrolyte dosage (mol L^{-1})	0.07
Inter-electrode distance (cm)	1
Initial concentration (mg L^{-1})	60
pH	7.8
Current density (mA cm^{-2})	15.5
Reaction time (min)	23
Chitosan dosage (g L^{-1})	0.7
Removal (%) (predicted)	99.71
Removal (%) (experimental)	100

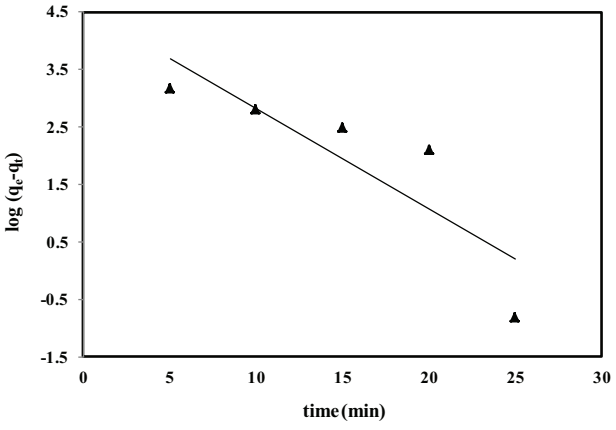

Fig. 9. First-order kinetic plot for CFZ removal in optimized EC/AD process condition.

Table 5
Kinetic models parameters for CFZ removal in optimized EC process condition

Second-order kinetic			First-order kinetic	
R^2	K_2 (g min mg^{-1})	q_e (mg g^{-1})	R^2	K_1 (min^{-1})
0.9715	4×10^{-5}	476.19	0.7414	0.400

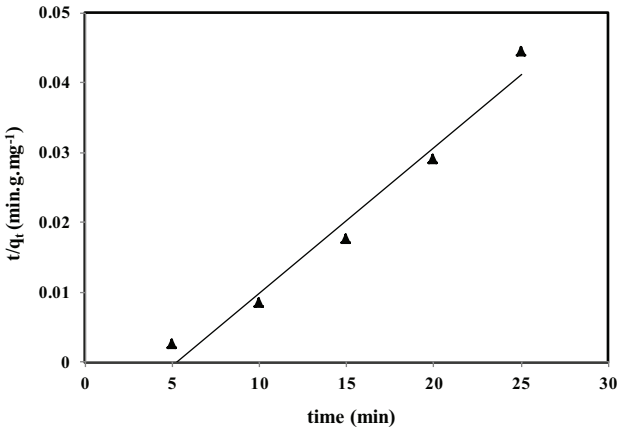

Fig. 10. Second-order kinetic plot for CFZ removal in optimized EC/AD process condition.

results are in good agreement with the second-order model in comparison with the first-order model for describing the kinetics of CFZ adsorption on $[Al(OH)_2]^+$.

3.8. Isotherm modeling

During the EC process, the metal hydroxides as the adsorbent were produced. The contaminants adsorption on the surface of the generated metal hydroxides investigated using two common adsorption isotherms namely Freundlich and Langmuir models. The model with the better appropriate correlation for the equilibrium curve could provide valuable information on the mechanism of the adsorption process.

To investigate the Freundlich isotherm, the used CFZ concentrations were 50–150 mg L^{-1} with the current density of 15.5 mA cm^{-2}, an initial pH of 7.8, and the chitosan dosage of 0.7 g L^{-1} in 25 min reaction time. It can be seen from Fig. 11, the correlation coefficient of the plot logq_e vs. logC_e is 0.9116. However, according to Fig. 12 the correlation coefficient of the plot C_e/q_e vs. C_e is 0.9851. The obtained intercept and slope denote the adsorption capacity and adsorption intensity, respectively. The calculated value of n from the slope of the plot falling in the range of 1–10 indicates favorable sorption. K_f and n values listed in Table 6.

The values of monolayer capacity (q_m), Langmuir constant (b), equilibrium constant (RL) and the correlation coefficient values of Langmuir and Freundlich isotherm models presented in Table 6. As it can be seen, the Langmuir isotherm model has higher regression coefficient compared with Freundlich model indicating that the Langmuir model provides a better description of the process. The obtained results suggested the monolayer adsorption of CFZ on the surface of the adsorbent and are in accordance with the Langmuirian

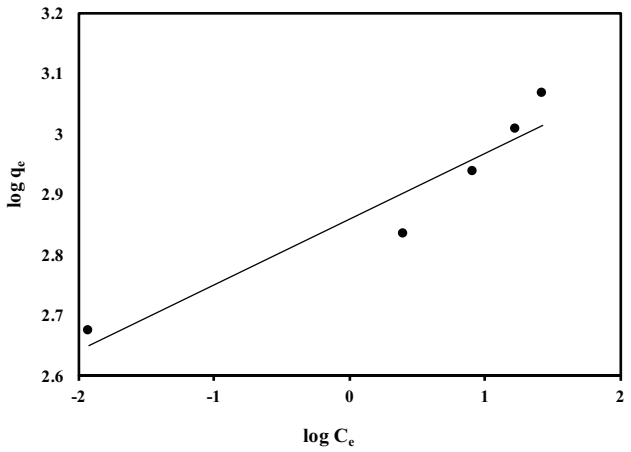

Fig. 11. Freundlich adsorption isotherm plot for CFZ removal in optimized EC/AD process condition.

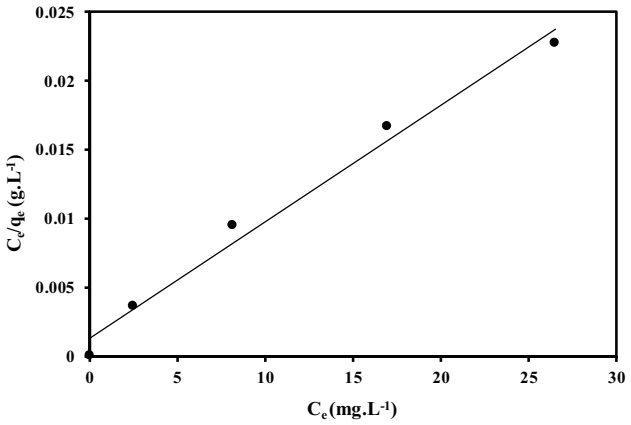

Fig. 12. Langmuir adsorption isotherm plot for CFZ removal in optimized EC/AD process condition.

Table 6
Langmuir and Freundlich adsorption isotherm models values for CFZ removal in optimized EC process condition

Langmuir isotherm				Freundlich isotherm		
q_m (mg g^{-1})	b (L mg^{-1})	RL	R^2	K_f	n	R^2
1,250	1.75	0.01	0.9851	723.76	9.17	0.9116

behavior of CFZ adsorption on aluminum hydroxide as described by previous researchers [28].

3.9. CFZ contaminant removal from hospital wastewater

A volume of 20 mL hospital wastewater was centrifuged at 1,500g for 15 min. The supernatant collected and a volume of 2.00 mL transferred into a 15 mL polypropylene centrifuge tube. A volume of 7.0 mL acetonitrile added and the mixture shaken strongly for 2 min. The mixture centrifuged at 1,500g for 10 min and the supernatant evaporated to 2 mL at 45°C–50°C under a steam of nitrogen [34]. The extract diluted with 20 mL of water and filtered by 0.22 μm polytetrafluoroethylene syringe filter to

inject into the HPLC system. The initial CFZ antibiotic concentration extracted from hospital wastewater sample were found to be 4.63 ± 0.13 mg L^{-1}, where reached to zero after applying the optimal condition of EC/AD process. However, applying each of the EC or AD techniques separately on the same sample resulted in 61% and 17% removal efficiency, respectively.

Moreover, to evaluate the removal efficiency of EC/AD process in high-concentration real samples, the proposed process was employed for treatment of 45 and 70 mg L^{-1} CFZ in hospital wastewater samples using standard addition method. The residual amount of CFZ in the treated samples was found to be 1.8 ± 0.21 and 6.3 ± 0.27 mg L^{-1}, which indicated satisfactory removal efficiency of 96% and 91%, respectively.

3.10. Evaluation of electrical energy and electrode consumption

The amount of aluminum electrode consumption during EC/AD process under optimal condition was found to be 0.024 g during a single run using Eq. (8). It can be concluded that, 96 g electrode consumed for treatment of 1 m^3 hospital wastewater. On the other hand, the amount of electrical energy consumption during EC/AD process under optimal condition was found to be 1.251 kWh m^{-3} using Eq. (9).

The amount of characteristic parameters including current efficiency (ϕ), weight loss of electrodes (ΔM_{exp}) during EC/AD process, the theoretical amount of electrodes dissolution (ΔM_{theo}) and SEEC were calculated and summarized in Table 7.

4. Conclusions

In the current work, the effects of experimental parameters such as initial CFZ concentration, solution pH, current density, reaction time, chitosan dosage, inter-electrode distance, type and concentration of electrolyte on the CFZ removal efficiency were investigated using EC/AD coupling process. The obtained results revealed that EC/AD coupling process was able to eliminate antibiotic CFZ effectively. Increasing current density and chitosan dosage demonstrated the most positive effect on the CFZ removal, whereas increasing of initial CFZ concentration can cause performance falling. Under optimal condition, electrode consumption and electrical energy consumption were found to be 0.024 g during a single run and 1.251 kWh m^{-3}, respectively. EC/AD coupling process followed both Langmuir and Freundlich isotherms; however, it was more adapted with the first one. The process kinetic successfully fitted to the second-order model. The developed process applied successfully for CFZ removal from hospital wastewater and the predicted model for treatment of synthetic wastewater is in satisfactory agreement with the removal efficiency of real hospital wastewater treatment.

Table 7
Electrical energy consumption values for CFZ removal in optimized process condition

M_{exp} (mg)	25.83
M_{theo} (mg)	24.43
ϕ (%)	105.7
SEEC kWh (kg Al)$^{-1}$	0.121

Acknowledgments

The authors express their appreciation to Neuroscience Research Center and Pharmaceutics Research Center both affiliated to Institute of Neuropharmacology, Kerman University of Medical Sciences, Kerman, Iran, for financial support of the current work.

References

[1] G.Z. Kyzas, J. Fu, N.K. Lazaridis, D.N. Bikiaris, K.A. Matis, New approaches on the removal of pharmaceuticals from wastewaters with adsorbent materials, J. Mol. Liq., 209 (2015) 87–93.
[2] C.-J. Wang, Z. Li, W.-T. Jiang, J.-S. Jean, C.-C. Liu, Cation exchange interaction between antibiotic ciprofloxacin and montmorillonite, J. Hazard. Mater., 183 (2010) 309–314.
[3] M. Aghazadeh, R. Ghotaslou, M.A. Rezaee, M.H. Moshafi, Z. Hojabri, F. Saffari, Determination of antimicrobial resistance profile and inducible clindamycin resistance of coagulase negative staphylococci in pediatric patients: the first report from Iran, World J. Pediatr., 11 (2015) 250–254.
[4] Y. Fasihi, F. Saffari, M.R.K. Ghahraman, D. Kalantar-Neyestanaki, Molecular detection of macrolide and lincosamide-resistance genes in clinical methicillin-resistant *Staphylococcus aureus* isolates from Kerman, Iran, Arch. Pediatr. Infect. Dis., 5 (2016) 1–5.
[5] D. Kalantar, M. Sh, M. Razavi, Emergence of imipenem resistance and presence of metallo-β-lactamases enzymes in multi drug resistant Gram negative bacilli isolated from clinical samples in Kerman, 2007-2008, J. Kerman Univ. Med. Sci., 17 (2010) 208–214.
[6] J. Berto, G.C. Rochenbach, M.A.B. Barreiros, A.X. Corrêa, S. Peluso-Silva, C.M. Radetski, Physico-chemical, microbiological and ecotoxicological evaluation of a septic tank/Fenton reaction combination for the treatment of hospital wastewaters, Ecotoxicol. Environ. Saf., 72 (2009) 1076–1081.
[7] G. Iskender, A. Sezer, I. Arslan-Alaton, F.G. Babuna, O. Okay, Treatability of cefazolin antibiotic formulation effluent with O_3 and O_3/H_2O_2 processes, Water Sci. Technol., 55 (2007) 217–225.
[8] Y.Y. Gurkan, N. Turkten, A. Hatipoglu, Z. Cinar, Photocatalytic degradation of cefazolin over N-doped TiO_2 under UV and sunlight irradiation: prediction of the reaction paths via conceptual DFT, Chem. Eng. J., 184 (2012) 113–124.
[9] N. Shaikh, J. Al Khowtair, G. Al Sulaiti, A. Nasser, F. Ummunnisa, Z. Ahmed, Y. Hassens, Cefazolin and coagulation disorder: a case report and review of literature, Qatar Med. J., 21 (2012) 54–55.
[10] A. Fakhri, S. Rashidi, M. Asif, I. Tyagi, S. Agarwal, V.K. Gupta, Dynamic adsorption behavior and mechanism of cefotaxime, cefradine and cefazolin antibiotics on CdS-MWCNT nanocomposites, J. Mol. Liq., 215 (2016) 269–275.
[11] K. Kümmerer, A. Henninger, Promoting resistance by the emission of antibiotics from hospitals and households into effluent, Clin. Microbiol. Infect., 9 (2003) 1203–1214.
[12] T. Schwartz, W. Kohnen, B. Jansen, U. Obst, Detection of antibiotic-resistant bacteria and their resistance genes in wastewater, surface water, and drinking water biofilms, FEMS Microbiol. Ecol., 43 (2003) 325–335.
[13] O. Sahu, B. Mazumdar, P.K. Chaudhari, Treatment of wastewater by electrocoagulation: a review, Environ. Sci. Pollut. Res., 21 (2014) 2397–2413.
[14] A. Amani-Ghadim, S. Aber, A. Olad, H. Ashassi-Sorkhabi, Optimization of electrocoagulation process for removal of an azo dye using response surface methodology and investigation on the occurrence of destructive side reactions, Chem. Eng. Process., 64 (2013) 68–78.

[15] S. Vasudevan, J. Lakshmi, G. Sozhan, Effects of alternating and direct current in electrocoagulation process on the removal of cadmium from water, J. Hazard. Mater., 192 (2011) 26–34.
[16] F. Ozyonar, S. Aksoy, Removal of salicylic acid from aqueous solutions using various electrodes and different connection modes by electrocoagulation, Int. J. Electrochem. Sci., 11 (2016) 3680–3696.
[17] M.M. Emamjomeh, M. Sivakumar, Review of pollutants removed by electrocoagulation and electrocoagulation/flotation processes, J. Environ. Manage., 90 (2009) 1663–1679.
[18] S. Ahmadzadeh, M. Rezayi, E. Faghih-Mirzaei, M. Yoosefian, A. Kassim, Highly selective detection of titanium (III) in industrial waste water samples using meso-octamethylcalix[4]pyrrole-doped PVC membrane ion-selective electrode, Electrochim. Acta, 178 (2015) 580–589.
[19] S. Ahmadzadeh, M. Rezayi, A. Kassim, M. Aghasi, Cesium selective polymeric membrane sensor based on *p*-isopropylcalix[6]arene and its application in environmental samples, RSC Adv., 5 (2015) 39209–39217.
[20] A. Pardakhty, S. Ahmadzadeh, S. Avazpour, V.K. Gupta, Highly sensitive and efficient voltammetric determination of ascorbic acid in food and pharmaceutical samples from aqueous solutions based on nanostructure carbon paste electrode as a sensor, J. Mol. Liq., 216 (2016) 387–391.
[21] M. Rezayi, R. Karazhian, Y. Abdollahi, L. Narimani, S.B.T. Sany, S. Ahmadzadeh, Y. Alias, Titanium (III) cation selective electrode based on synthesized tris(2pyridyl) methylamine ionophore and its application in water samples, Sci. Rep., 4 (2014) 1–8.
[22] H. Soltani, A. Pardakhty, S. Ahmadzadeh, Determination of hydroquinone in food and pharmaceutical samples using a voltammetric based sensor employing NiO nanoparticle and ionic liquids, J. Mol. Liq., 219 (2016) 63–67.
[23] M. Fouladgar, S. Ahmadzadeh, Application of a nanostructured sensor based on NiO nanoparticles modified carbon paste electrode for determination of methyldopa in the presence of folic acid, Appl. Surf. Sci., 379 (2016) 150–155.
[24] M. Doltabadi, H. Alidadi, M. Davoudi, Comparative study of cationic and anionic dye removal from aqueous solutions using sawdust-based adsorbent, Environ. Prog. Sustain. Energy, 35 (2016) 1078–1090.
[25] M. Kobya, E. Demirbas, Evaluations of operating parameters on treatment of can manufacturing wastewater by electrocoagulation, J. Water Process Eng., 8 (2015) 64–74.
[26] M.H. Dehghani, A. Dehghan, H. Alidadi, M. Dolatabadi, M. Mehrabpour, A. Converti, Removal of methylene blue dye from aqueous solutions by a new chitosan/zeolite composite from shrimp waste: kinetic and equilibrium study, Korean J. Chem. Eng., 34 (2017) 1699–1707.
[27] S. Ahmadzadeh, A. Asadipour, M. Pournamdari, B. Behnam, H.R. Rahimi, M. Dolatabadi, Removal of ciprofloxacin from hospital wastewater using electrocoagulation technique by aluminum electrode: optimization and modelling through response surface methodology, Process Saf. Environ. Prot., 109 (2017) 538–547.
[28] M.S. Secula, B. Cagnon, T.F. de Oliveira, O. Chedeville, H. Fauduet, Removal of acid dye from aqueous solutions by electrocoagulation/GAC adsorption coupling: kinetics and electrical operating costs, J. Taiwan Inst. Chem. Eng., 43 (2012) 767–775.
[29] S. Ahmadzadeh, A. Kassim, M. Rezayi, G.H. Rounaghi, Thermodynamic study of the complexation of *p*-isopropylcalix[6] arene with Cs^+ cation in dimethylsulfoxide-acetonitrile binary media, Molecules, 16 (2011) 8130–8142.
[30] S. Ahmadzadeh, M. Rezayi, H. Karimi-Maleh, Y. Alias, Conductometric measurements of complexation study between 4-isopropylcalix[4]arene and Cr^{3+} cation in THF-DMSO binary solvents, Measurement, 70 (2015) 214–224.
[31] M. Yoosefian, S. Ahmadzadeh, M. Aghasi, M. Dolatabadi, Optimization of electrocoagulation process for efficient removal of ciprofloxacin antibiotic using iron electrode; kinetic and isotherm studies of adsorption, J. Mol. Liq., 225 (2017) 544–553.
[32] A.K. Yadav, L. Singh, A. Mohanty, S. Satya, T. Sreekrishnan, Removal of various pollutants from wastewater by electrocoagulation using iron and aluminium electrode, Desal. Wat. Treat., 46 (2012) 352–358.
[33] W.-L. Chou, C.-T. Wang, K.-Y. Huang, T.-C. Liu, Electrochemical removal of salicylic acid from aqueous solutions using aluminum electrodes, Desalination, 271 (2011) 55–61.
[34] L.K. Sørensen, L.K. Snor, Determination of cephalosporins in raw bovine milk by high-performance liquid chromatography, J. Chromatogr., A, 882 (2000) 145–151.